Journal of Signal and Image Processing
ISSN: 0976-8882 & E-ISSN: 0976-8890, Vol. 2, Issue 1, 2011, pp-26-35
Available online at http://www.bioinfo.in/contents.php?id=48

MULTIWAVELET TRANSFORMATION FOR SAR IMAGE CODING: PERFORMANCE EVALUATION FOR LOSSY COMPRESSION

MAGAR G.M.[1], GORNALE S.S.[2*] AND KALE K.V.[1]
Department of CS & IT, Dr. B. A. Marathwada University, Aurangabad - 431004, India
Department of Computer Science, Government College (Autonomous), Mandya, India
*Corresponding author. E-mail: shivanand_gornale@yahoo.com

Received: July 08, 2011; Accepted: August 13, 2011

Abstract- Synthetic Aperture Radar (SAR) System generates the large volume of the data and the ability to transmit it to the ground, or to store it, is not increasing as fast, due to practical constraints imposed in the system design. This shortfall prompts interest in compression-decompression strategies for rapid transmission of images. Transform coding based on the Discrete Cosine Transform (DCT), and the Discrete Wavelet Transform (DWT) is well understood for optical images but has not been well studied for SAR Images. Wavelets have been introduced as a signal-processing tool and they are widely used in image compression applications. The transform in wavelet and multiwavelet domain is capable of compacting the energy of image into a small number of coefficients, localized in both space and frequency. But the wavelet transform has got more importance due to its manifold characteristics i.e. high compression ratio, multi-resolution in nature, use of different basis functions that lead to the desirable property of characterizing and localizing signal features in frequency domains. In this paper, we have evaluated the performance of Discrete Cosine Transform, Block Truncation Coding (BTC), Gaussian Pyramidal (GP) and Multiwavelet Transformation (MWT). Mean squared Error (MSE), Maximum Absolute Error (MAE), Signal to Noise Ratio (SNR), Peak signal to noise ratio (PSNR), Compression Ratio (CR), is used as objective performance criteria. Based on the observation of the above performance evaluation system, the promising result has been depicted i.e on an average compression 70% to 77% and RE 96.Objective of exploiting features MWT for compression of SAR images has been shown.
Keywords- Discrete Wavelet Transform (DWT), Gaussian Pyramidal Coding, Mutiwavelet Transform (MWT), Synthetic Aperture Radar (SAR)

Introduction

The Synthetic Aperture Radar (SAR) images play an important role in many applications including ecology, geology, surveillance, oceanography, glaciology, and agriculture. SAR images can provide unique information about the surface of the Earth by using the motion of a satellite or an airplane they are mounted on [1,2,3,4].SAR has ability to penetrate the cloud cover and doesn't depends on any external source of the energy like sun rays. With the improvement of SAR technology, larger areas are imaged and higher resolution sensors are considered for many applications. This causes the volume of data associated with SAR images to be extremely large, thus effective compression of SAR images is highly required in order to reduce the burden of storage and transmission. There are some special characteristics of SAR imagery that differentiate it from normal optical images. The first is the speckle noise phenomenon due to the coherence of radar radiation and the multi-look nature of SAR images [5-11]. Speckle noise represents the most significant noise in SAR images. The second is that there are large homogeneous regions as well as detailed texture information in SAR images. Synthetic Aperture Radar (SAR) instruments transmit radar signals and then measures how strongly the signals are scattered back. A single antenna moving along the flight line acquires the data and the effect is similar to using an array of antennas. The target is illuminated several times from different locations generating numerous echoes that are recorded coherently (i.e., amplitude and phase as a function of time) and subsequently combined to synthesize a linear array. A higher spatial resolution is achieved independently of the distance between sensor and target and by a small antenna. One of the major constraints in the design and operation of current SAR systems is the unavailability of a downlink with a high data rate. The data rate of each channel is proportional to the pulse repetition frequency, the number of sampled values in each received echo, and the number of quantization bits in each sample. Since reducing the data rate deteriorates the system performance, data compression is required. Radar system produces a mass of data for objects imaging. However, with the rapidly increasing data collection capacity, its ability to transmit and store data is relatively weaker. Many measures can reduce data rate while depressing the whole running effect of the system. For instance, reducing pulse repeating frequency would introduce blurred azimuth and reduced azimuth resolution unless the system use longer azimuth

antenna. Also, reducing range resolution would depress system bandwidth. Only to simply reduce quantified bits would increase digitized noise, and as a result damage the pulse response function, image dynamic range and radiation accuracy [12,13]. Therefore, in order to improve SAR system, data compression algorithms with high efficiency have become an important objective.

Principles of Transform Coding

A general transform coding scheme involves subdividing an NxN image into smaller nxn blocks and performing a unitary transform on each sub image [14-17]. A unitary transform is a reversible linear transform whose kernel describes a set of complete, orthonormal discrete basic functions. Typical examples are transform-coding methods, in which the data is represented in a different domain (for example, frequency in the case of the Fourier Transform [FT], the Discrete Cosine Transform [DCT], the Kahrunen-Loewe Transform [KLT], and so on)[18-21], where a reduced number of coefficients contain most of the original information. In many cases this first phase does not result in any loss of information. The aim of quantization is to reduce the amount of data used to represent the information within the new domain. Quantization is in most cases not a reversible operation: therefore, it belongs to the so-called 'lossy' methods. Data compression algorithms can be classified as lossless and lossy [18]. Lossless compression algorithms such as Huffman coding, arithmetic coding, run-length encoding, and Lempel-Ziv coding are used when exact reconstruction of the original data set is necessary. Lossy compression algorithms such as predictive coding, transform/ subband coding, vector quantization, and fractal coding are used for applications in which some degree of degradation of the data is tolerable and/or high compression ratio is preferred [18-24, 37].

Discrete Cosine Transform

The 1-D *discrete cosine transform* (DCT) is defined as

$$C(u) = \alpha(u) \sum_{x=0}^{N-1} f(x) \cdot \cos\left[\frac{(2x+1)u\pi}{2N}\right] \quad (1)$$

Similarly, the inverse DCT is defined as

$$f(x) = \sum_{u=0}^{N-1} \alpha(u) C(u) \cdot \cos\left[\frac{(2x+1)u\pi}{2N}\right] \quad (2)$$

Where

$$\alpha(u) = \begin{cases} \sqrt{1/N} & \text{for} \quad u = 0 \\ \sqrt{2/N} & \text{for} \quad u = 1,2,\ldots,N-1 \end{cases} \quad (3)$$

The corresponding 2-D DCT, and the inverse DCT are defined as

$$C(u,v) = \alpha(u)\alpha(v) \sum_{x=0}^{N-1}\sum_{y=0}^{N-1} f(x,y) \cdot \cos\left[\frac{(2x+1)u\pi}{2N}\right] \cdot \cos\left[\frac{(2y+1)v\pi}{2N}\right] \quad (4)$$

and

$$f(x,y) = \sum_{u=0}^{N-1}\sum_{v=0}^{N-1} \alpha(u)\alpha(v)C(u,v) \cdot \cos\left[\frac{(2x+1)u\pi}{2N}\right] \cdot \cos\left[\frac{(2y+1)v\pi}{2N}\right] \quad (5)$$

The advantage of DCT is that it can be expressed without complex numbers. 2-D DCT is also separable (like 2-D Fourier transform), i.e. it can be obtained by two subsequent 1-D DCT in the same way as Fourier Transform. For analysis of two-dimensional (2D) signals such as images, we need a 2D version of the DCT. For an *n* x *m* matrix C, the 2D DCT is computed in a simple way: The 1D DCT is applied to each row of C and then to each column of the result. Since the 2D DCT can be computed by applying 1D transforms separately to the rows and columns, we say that the 2D DCT is *separable* in the two dimensions.

Multiwavelet

The basic idea to wavelets is to analyze (a signal) according to scale. Multiwavelets constitute techniques, which have been added to wavelet theory in recent years [25-34].Many authors tried to exploits wavelet domain techniques for SAR image processing applications [35-36]. Recently, much interest has been generated in the study of the multiwavelets, where more than one scaling function and mother wavelet are used to represent a given signal. In the wavelet and other transform coding bases function is single and does not change, but in multiwavelets multiple basis function is possible [38-51]. In contrast to the limitations of scalar wavelets, multiwavelets are able to possess the best of all these properties simultaneously. Second, one desirable feature of any transform used in image compression is the amount of energy compaction achieved. A filter with good energy compaction properties can decorrelate a fairly uniform input signal into a small number of scaling coefficients containing most of the energy and a large number of sparse wavelet coefficients. This becomes important during quantization since the wavelet coefficients are typically represented with significantly fewer bits on average than the scaling coefficients.

Multiscaling functionality in the Multiwavelet

Multiwavelets are characterized with several scaling functions and associated wavelet functions. Let the scaling functions be denoted in vector form as $\Phi(t) = [\Phi_1(t), \Phi_2(t), \ldots, \Phi r(t)]^T$, where $\Phi(t)$ is called the multiscaling function, T denotes the vector transpose and $\Phi_j(t)$ is the j^{th} scaling function. Likewise, let the wavelets be denoted as $\Psi(t) = [\psi_1(t), \psi_2(t), \ldots, \psi_r(t)]^T$, where $\psi_j(t)$ is the j^{th} wavelet function. Then, the dilation and wavelet equations for Multiwavelet take the following forms, respectively:

$$\phi(t) = \sum_{k}^{r} Hk \ \phi(2t - k),$$
$$\psi(t) = \sum_{k}^{r} Gk \ \phi(2t - k) \quad (6)$$

Multiwavelet bases of multiplicity r provide a multi-resolution analysis is $\{V_n\}_{n \in Z}$ of $L^2(R)$ using the Multiwavelet function Ψ(t) and multiscaling function Φ(t).

The j^{th} scaling space is given by

$$V_j = \overline{span\{2^{j/2}\phi_i(2^j.t-k) : 1 \le i \le r, k \in Z\}} \quad (7)$$

The jth wavelet space is given by

$$W_j = \overline{span\{2^{j/2}\psi_i(2^j.t-k) : 1 \le i \le r, k \in Z\}} \quad (8)$$

Where $V_j \perp W_j$. The multi scaling function satisfied the above r-scale equation (6). Where H_k and Gk are r x r matrix coefficients of low pass multifilters and high pass multifilters. The low pass filters H and the high pass filter G is r x r matrix filters, instead of scalars. In theory, r could be as large as possible, but in practice it is usually chosen to be two i.e r =2 [10, 32].

The wavelet transform has proved to be an efficient tool for many image processing applications. By means of lowpass and highpass filters, at each step, the image (or an approximation of the image), belonging to a subspace V_j , is decomposed into its projection onto 2 subspaces: an approximation subspace V_{j-1} and a detail subspace W_{j-1}, both having less resolution. When the process is completed, the image is represented as the sum of its details at different resolutions and positions, plus a coarse approximation of the same image. The approximation subspaces V_j , which are nested, are the linear span of the scaling function Φ (or a scaled version of Φ) and its integer translates. The detail subspaces W_j are the linear span of the wavelet Ψ (or a scaled version of Ψ) and its integer translates. We call (Φ, Ψ) a wavelet system. In one dimension, the different scales are powers of a dilation factor, most commonly equal to 2. To process an image, the tensor product of one-dimensional filters is used; the details lie mainly in the vertical and horizontal directions, which does not agree with our visual system Multiwavelets, related to time–varying filterbanks, are a generalization of the wavelet theory, in which the approximation subspaces V_j are the linear span of more than one scaling function. They offer a greater degree of freedom in the design of filters. The Multiwavelet used here has two channels, so there will be two sets of scaling coefficients and two sets of wavelet coefficients. Thus the two-dimensional image data, after one level multiwavelet decomposition are replaced by sixteen blocks corresponding to the subbands. The sixteen blocks represent either low pass or high pass filtering in each direction, not four blocks in scalar wavelet decomposition. For two-level multiwavelet decomposition, the four low frequency subbands are decomposed into sixteen blocks again.

Compression Method

The primary goal is to apply the multiwavelets on the image with prefiltering and observe the perceptual quality of the image. Applying the multiwavelets successively on the decomposed image and measure the performance. We retain the same number of largest coefficients for each multiwavelet, and then invert the algorithm to reconstruct the image and measure the performance of each multiwavelet by assessment criteria. One of the major tasks in realizing multiwavelets is, using the efficient prefilter in the processing. In the case of scalar wavelets, the given signal data are usually assumed to be the scaling coefficients that are sampled at a certain resolution, and hence, we directly apply multi-resolution decomposition on the given signal. But the same technique cannot be employed directly in the multiwavelet setting and some prefiltering has to be performed on the input signal prior to multiwavelet decomposition. The type of the prefiltering employed is critical for the success of the results obtained in application. And therefore selection of the best prefilter becomes the big challenge for the different characteristic images. A simple threshold compression method has been applied based on the following steps:

1) Apply the prefiltering techniques on the image
2) Apply the multiwavelets
3) Reconstruct the image by inverse transformation, keeping the largest number of the coefficient.
4) Decompose the image and repeat the step 1 and 3, keeping the largest number of the coefficient.

Assessment Criteria

An SAR image compression algorithm is judged by its ability to minimize the distortion while retaining all significant features of the image. The distortion in reconstruction has been computed by means of the following formula:

The mean square error is one of the most commonly used performance measures in image and signal processing. For an image of size NxM it can be defined as

$$MSE = \frac{1}{NM} \sum_{n=0}^{N-1} \sum_{m=0}^{M-1} [x(n,m) - \hat{x}(n,m)]^2 \quad (9)$$

Where x (n, m), $\hat{x}(n,m)$ are original and decompressed image respectively.

Signal to Nose Ratio (SNR)

$$\mathrm{SNR} = 10 \log 10 \ \frac{1}{NMSE} \quad (10)$$

Peak Signal to noise ratio (PSNR)

$$\mathrm{PSNR} = 10 \log 10 \frac{(\text{peak} - \text{to} - \text{peak value of original image})^2}{\mathrm{MSE}} \quad (11)$$

Maximum Absolute Error (MAE)

Maximum absolute error shows the worst-case error occurring in the compressed image.

$$\mathrm{MAE} = \max_{0<=m,n<=N-1} |x(m,n) - \hat{x}(m,n)| \quad (12)$$

Retain Energy (RE)

$$RE = \frac{100 * (\mathrm{vn}(\mathrm{ccd},2))^2}{(\mathrm{vn}(\mathrm{originalsignal}))^2} \quad (13)$$

Where vn is the vector norm, ccd is the coefficients of the current decomposition [30].

Compression Ratio

$$CR = \frac{\text{size of the original files(byte)}}{\text{size of the compressed files(byte)}} \quad (14)$$

Experimental results and Discussion

Experiments are performed with a radar image acquired by the Spaceborne Imaging Radar-C/X-Band Synthetic Aperture Radar (SIR- C/X-SAR) aboard the space shuttle Endeavour on October 9, 1994. The colors are assigned to different frequencies and polarizations of the radar as follows: Red is L-band vertically transmitted, vertically received; green is the average of L-band vertically transmitted, vertically received and C-band vertically transmitted, vertically received; blue is C-band vertically transmitted, vertically received. The image is located at 19.25 degrees north latitude and 71.34 degrees east longitude and covers an area 20 km by 45 km (12.4 miles by 27.9 miles). We have used 256×256 sc-lval4.jpg image characteristics to demonstrate the performance of the system.

Frequency domain techniques like DCT, BTC, GP are used for decomposing and reconstruction of the SAR image. Multiwavelet domain techniques (MWT) like haar, d4, la8, bi9, bi7, bi5, bi3, cl, sa4, bighm6 are used for decomposing the SAR image. Prefiltering is done by using multiwavelets transform namely bih5ap. The biorthogonal multiwavelet transformation bighm6 is used in the reconstruction. The SAR image data is normalized so that the minimum and maximum pixel values are 0 and 1, respectively and processing is done. Resultant data of each transformation are tabulated in the Table 1, Table 2 respectively. Corresponding graphs are also used for the interpretation and visual perception of the SAR image as indicated in the figures (fig. 1(a-c), fig.2(a-o) and fig.3(a-z, aa-ab). Based on this data collected from the different techniques performance for the compression is measured using the assessment criteria. We have observed that the reconstructed image with these multiresolution techniques for decomposition and reconstruction yielded the highest perceptual quality, high PSNR and good compression. We have observed that size of the compressed file decreases as the decomposition level increases from level-1 to level-5, but the visual quality of the image also degrades. So it indicates that as the image is decomposed for the more levels, in each step the more detail coefficient of the image will be losing and it results in reduction of the image size. Performance of multiwavelet transformation techniques is very well in terms of human visual impact so as to interpretation and analysis of the SAR image. The variation in the MSE and PSNR are the noticeable point at different decomposition level. Less MSE indicates the best visual quality. If we increase the level of decomposition the computational complexity will increase. At decomposition level-1, biorthogonal multiwavelet transforms bi3 and bighm6 gives good compression as well as good visual quality. At decomposition level-2, sa4 and bighm6 gives excellent variation in the compression. From Decomposition level-3 to level-5 all multiwavelet transformation haar,d4,la8,bi9,bi7,bi5,bi3,cl,sa4,bighm6 gives good compression ratio but there is variation in the visual quality of the SAR image.

Conclusion

Based on the experimental work carried by using the DCT, BTC, GP and MWT transformations, we got the highest compression by using biorthogonal multiwavelets bighm6 at decomposition level-4 and level-5 i.e. 70.84% and 77.87% respectively.

Performance of above transformation techniques has been evaluated through human visual impact and objective methods (MSE, PSNR, CR). Less MSE indicates the good quality of image. However the variation in the MSE and PSNR are the noticeable point at different decomposition level. If we increase the level of decomposition the computational complexity will increase. So it is concluded that, multiscaling functionality of multiwavelet transformation can be exploited for lossy compression of SAR image. It reduces the computational complexity and gives promising results.

References

[1] Wei D., Guo H., Odegard J., Lang M. and Burrus C., (1995) *SPIE Conference on Wavelet Applications, Vol. 2491, Orlando, FL*.

[2] Fatma A. Sakaya, Dong Wei Serkan Emek (1997) *Proceedings of the 1997 IEEE International Conference on Acoustics, Speech, and Signal Processing (ICASSP '97)*.

[3] Cumming J. Wang (2002) *IEEE Transaction on Geoscience and Remote Sensing Symposium*, Vol-2,pp- 1126- 1128.

[4] Wang Wen, Xing Fu-cheng, Dong Yun-long and Rui Guo-sheng (2005) *IEEE International Symposium on Microwave, Antenna, Propagation and EMC Technologes for Wireless Communications Proceedings.*

[5] Xingsong Hou, Guizhong Liu and Yiyang Zou (2004) *IEEE Transactions On Geoscience And Remote Sensing*, Vol. 42, No. 11.

[6] Dohono D.L. , (1933) *IEEE Transactions Information Theory*, No. 3, PP: 933-936.

[7] Grace Chang S., Bin Yu and Vattereli M. (2000) *IEEE Transactions on Image Processing*, Vol. 9, PP: 1532-1546.

[8] Grace Chang S., Bin Yu and Vattereli M. (2000) *IEEE Transactions on Image Processing*, Vol. 9, PP: 1522-1530.

[9] Panda G., Meher S.K. & Majhi B. (2000) *Journal of the CSI* 30, 3.

[10] Mvogo J., Mercier G., Onana V.P., Rudant J.P., Tonye E., Trebossen École H. (2001) *IEEE International Symposium on Geoscience and Remote Sensing* , Vol.1, PP: 103-105.

[11] Buades A., et. Al (2005) *Simulation* Vol 4, No. 2, PP:496-530.

[12] Andreas Reigber (2005) *IEEE Geoscience And Remote Sensing Letters*, Vol. 2, No. 1, , Pp45-49.

[13] Guner Arslan and Magesh Valliappan (1998) *Multidimensional Signal Processing*.
[14] Raz J. and Turetsky B. (1999) *Proc. SPIE,vol. 3813, Wavelet Applications in Signal and Image Processing*, pp.561–570.
[15] Hervet E., Fjørtoft R., Marthon P. and Lop`es A. (1998) *SAR Image Analysis, Modelling and Techniques III,* vol. SPIE-2497.
[16] Gornale S.S., Vikas Humbe, Manza R.R., Kale K.V. (2006) *International Conference on Systemics, cybernetics and informatics*, PP. 830-835.
[17] Zahn R. (2003) *IEEE Transactions Proceeding of Radar Sonar and Navigation*, Volume 150, Issue 3, 2, 104 - 112.
[18] Jun ZHANG, Yingjun HUANG, Hao TIAN, Lin LIAN, (2007) *1st Asian and Pacific Conference on Synthetic Aperture Radar*, 671-674.
[19] Rafael C. Gonzalez and Richard E. Woods (2001) *Digital Image Processing, 2nd edition", Prentice Hall*.
[20] Subhasis Saha. *Image Compression - from DCT to Wavelets: A Review, ACM Student Magzine*.
[21] Jain A.K. (1989) *Fundamentals of Digital Image Processing, Upper Saddle River, NJ: Prentic Hall*.
[22] DuSan Gleich, Peter PlaninSiE, Bojan GergiE, Boris Banjanin, Karko & Eej (1999) *ISIE'99 - Bled, Slovenia*.
[23] Kwon Kim, Rue-Hong Park (1998) *IEEE International Conference on Acoustics, Speech, and Signal Processing*, 5, 2625-2628.
[24] James W. Owens, Michael W. Marcellin, Bobby R. Hunt, and Marvin Kleine (1997) *Proceedings of the 1997 International Conference on Image Processing (ICIP '97)*.
[25] Cumming J. Wang (2002) *IEEE International Symposium on Geoscience and Remote Sensing*, 2, PP: 1126- 1128.
[26] Kim B.S., Yoo S.K., Lee M.H. (2006) *IEEE Transactions on Information Technology in Biomedicine*, Volume 10, Issue 1, 77 - 83.
[27] Sarshar N., Wu X. (2007) *IEEE Transactions on Image Processing*, Volume 16, Issue 5, 1383 - 1394.
[28] Ingrid Daubechies (1990) *IEEE transactions on information theory*, 36(5): 961-1005.
[29] Junejo N., Ahmed N., Unar M.A., Rajput A.Q.K. (2005) *IEEE/Sarnoff Symposium on Advances in Wired and Wireless Communication*, 45 – 48.
[30] Gornale S.S., Vikas Humbe, Manza R.R., Kale K.V. *International Journal of Computer Science and Security*, Volume 1: Issue (2).
[31] Li Ke, Qiang Du (2007) *International Conference on Computational Intelligence and Security Workshops,China.*
[32] Wang Ling (2000) *5th International Conference on Signal Processing Proceedings*, *WCCC-ICSP 2000*, Volume: 2, page(s): 987-991.
[33] Wang Zhenhua, Xu Hondgbo, Tian Yan, Tian Jinwen, Liu Jian (2002) *Processing and Intelligent Control, Wuhan 430074, China, ICSP'02 Proceedings*.
[34] Ian Cumming and Jing Wang (2003) *Proceedings of the Data Compression Conference (DCC'03).*
[35] Gregoire Mercier, Marie-Catherine Mouchot, and Guy Cazuguel (1998) *Proceedings of the 1998 International Conference on Image Processing (ICIP '98).*
[36] Zhaohui Zeng and Ian Cumming (1998) *Proceedings of ICSP '98.*
[37] Robi Polikar, The Wavelet Tutorial,Part IV, http://users.rowan.edu/~polikar/WAVELETS/WTpart4.html
[38] Goodman T.N.T. and Lee S.L. (1994) *Trans. Amer. Math. Soc.*, vol. 342, pp. 307–324.
[39] Cotronei M., Montefusco L. B. and Puccio L. (1998) *IEEE Trans. Circuits Syst*. II, vol. 45, no. 8, pp. 970–985.
[40] Strela V. (1996) *Multiwavelets: theory and applications, Ph.D. thesis, Massachusetts Institute of Technology, Boston, Mass, USA*.
[41] Hardin D. P. and Roach D. (1998) *IEEE Trans. Circuits Syst*. II, vol. 45, no. 8, pp. 1106–1112.
[42] Strela V., Heller P., Strang G., Topiwala P. and Heil C. (1999) *IEEE Trans. Image Processing*, vol. 8, no. 4, pp. 548–563.
[43] Geronimo J., Hardin D. and Massopust P. R. (1994) *J. Approx. Theory*, vol. 78, no. 3, pp. 373–401.
[44] Shen L., Tan H.H. and Tham J.Y. (2000) *Appl. Comput.Harmon. Anal.*, vol. 8, no. 3, pp. 258– 279.
[45] Chui C. K. and Lian J. A. (1995) *Cat report 351, Texas A&M University, Texarkana, Tex, USA*.
[46] Tham J.Y., Shen L., Lee S.L. and Tan H. H. (2000) *IEEE Trans. Signal Processing*, vol. 48, no. 2, pp. 457–464.
[47] Selesnick I. W. (1999) *IEEE Trans. Signal Processing*, vol. 47, no. 6, pp. 1615–1621.
[48] Selesnick I.W. (1998) *IEEE Trans. Signal Processing*, vol. 46, no. 11, pp. 2898–2908.
[49] Shen L., Tan H.H. and Tham J.Y. (2000) *IEEE Trans. Signal Processing*, vol. 48, no. 7, pp. 2161–2163.
[50] Strela V. (1998) *ContemporaryMathematics, A. Aldroubi and E. B. Lin, Eds.,* vol. 216, pp. 149–157.

CT: Compression Techniques
Table I-Shows the Compression of SAR Image in percentage for DCT, BTC and GP

CT	DL	SNR	PSNR	RE	CR	MSE	MAE	**Compression %**
DCT	-	27.31896	18.41867	99.9647	2.79901	0.01439	0.67718	64.27304
BTC(4x4)	-	57.23163	21.52011	99.9704	1.03552	0.00705	0.50588	3.42992
GP	-	18.98422	16.99172	98.8729	2.55576	0.01999	0.73333	60.87269

Table II- Shows the Compression of SAR Image in percentage for MWT

MWT	DL	SNR	PSNR	RE	CR	MSE	MAE	Compression %
haar	1	4.90512	10.75287	98.5642	1.05598	0.08408	1.33783	5.30117
	2	3.87420	9.99447	99.9004	1.69524	0.10013	1.04752	41.01124
	3	2.71307	8.59836	99.0098	2.24568	0.13809	1.04311	55.47014
	4	3.28083	9.50658	99.1487	2.62752	0.11203	1.03032	61.94137
	5	3.23824	9.67072	95.4534	2.94783	0.10788	0.92776	66.07671
d4	1	5.04700	10.89771	98.2155	1.06290	0.08133	1.38838	5.91788
	2	3.90894	10.07297	98.8153	1.68390	0.09833	1.05939	40.61418
	3	2.56069	8.40576	97.2635	2.24080	0.14435	1.09103	55.37298
	4	3.04391	9.44469	92.6699	2.61591	0.11364	1.07930	61.77241
	5	2.33560	8.82197	83.7749	2.80564	0.13116	0.95372	64.35752
la8	1	4.78177	10.79997	94.7189	1.06257	0.08318	1.99610	5.88832
	2	2.60769	8.73308	89.2562	1.61652	0.13387	1.88796	38.13889
	3	1.27050	6.24544	78.5178	2.02654	0.23739	1.96077	50.65473
	4	0.79122	5.00839	66.5768	2.47042	0.31562	1.95600	59.52099
	5	0.33335	3.77101	37.9745	3.25237	0.41966	1.80363	69.25319
bi9	1	3.71121	9.73736	92.9306	1.02312	0.10623	2.00272	2.25986
	2	1.92280	7.68059	83.8720	1.59582	0.17059	1.72297	37.33632
	3	1.01865	5.59026	73.5877	1.98358	0.27604	1.79238	49.58604
	4	0.58045	4.68539	52.7282	2.41547	0.33999	1.81712	58.60015
	5	0.14390	3.45657	17.3578	3.27759	0.45117	1.56734	69.48974
bi7	1	3.90900	10.00430	93.3460	1.07020	0.09990	1.85576	6.55994
	2	1.89711	7.51705	85.0618	1.55709	0.17713	1.79066	35.77765
	3	1.01937	5.40277	75.7917	1.92848	0.28822	1.85317	48.14565
	4	0.60509	4.52806	56.3446	2.38529	0.35253	1.80159	58.07637
	5	0.16247	3.25704	20.3671	3.25192	0.47238	1.61466	69.24897
bi5	1	3.48742	8.80835	98.0660	0.87825	0.13157	2.22859	-13.86331
	2	2.90410	8.58664	95.7723	1.30493	0.13846	2.17500	23.36741
	3	1.69634	6.70608	90.0768	1.90305	0.21350	2.25797	47.45290
	4	1.14189	5.79486	76.3184	2.59214	0.26334	1.90977	61.42181
	5	0.63059	4.21230	63.3451	3.36757	0.37911	1.97212	70.30498
bi3	1	4.34608	10.96587	79.0717	1.64311	0.08006	1.60645	39.13998
	2	3.59004	10.11190	91.4797	1.88427	0.09746	1.73797	46.92912
	3	1.77578	7.54806	83.2289	2.02066	0.17587	1.93321	50.51111
	4	1.14482	6.43671	70.1976	2.18516	0.22716	1.70855	54.23672
	5	0.55724	4.72865	50.8857	2.54177	0.33662	1.91759	60.65726
cl	1	4.62771	10.44071	94.9160	0.99865	0.09035	1.61102	-0.13517
	2	4.99336	11.19173	99.1507	1.89939	0.07600	0.96076	47.35152
	3	3.07259	9.15369	98.7782	2.15238	0.12152	1.00492	53.53975
	4	2.92181	9.08895	96.4340	2.30449	0.12334	1.01627	56.60640
	5	3.07601	9.46682	94.7206	2.43510	0.11306	0.99179	58.93385
sa4	1	8.68441	13.46043	97.0326	1.49193	0.04508	1.30929	32.97288
	2	6.28101	12.11146	99.6942	1.73246	0.06150	1.10624	42.27845
	3	4.15100	10.39649	99.3332	1.96383	0.09127	1.07047	49.07916
	4	2.67392	8.55005	99.6855	2.19753	0.13964	1.00261	54.49438
	5	2.74146	8.84953	96.7485	2.47558	0.13033	1.17195	59.60547
bighm6	1	15.45442	16.01531	99.6370	1.53409	0.02503	0.84272	34.81456
	2	14.89749	15.95320	99.1535	2.47662	0.02539	0.80452	59.62237
	3	12.01382	15.05948	99.0481	3.13854	0.03119	0.80488	68.13804
	4	9.81978	14.20490	100.1642	3.42903	0.03798	0.81815	70.83721
	5	7.05364	12.99185	96.1499	4.51880	0.05021	0.78366	77.87024

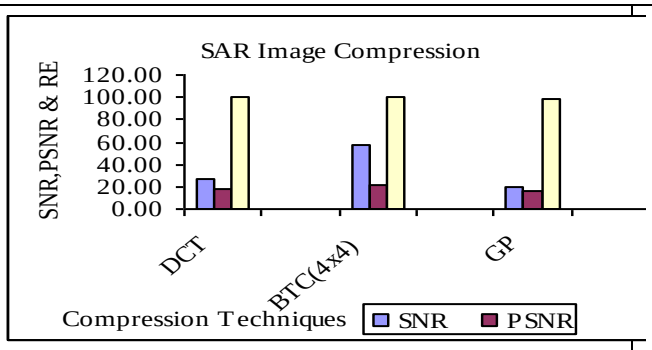

Fig. 1. (a) SNR, PSNR & RE

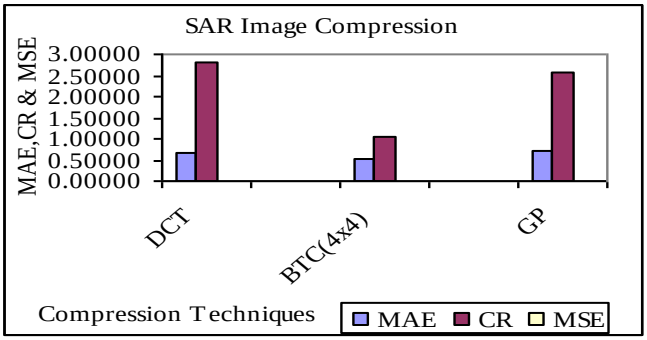

Fig. 1. (b) MAE, CR & MSE

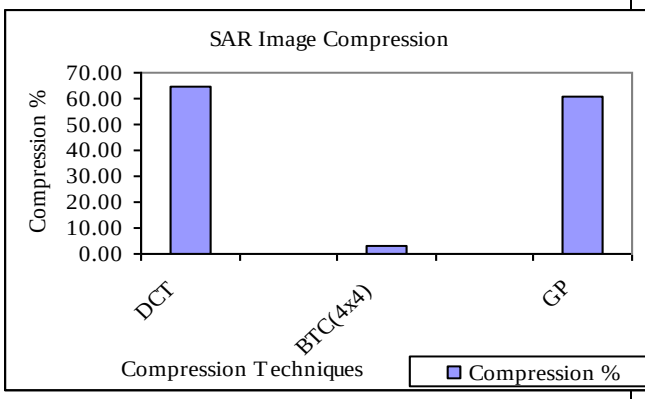

Fig 1. (c) Compression in %

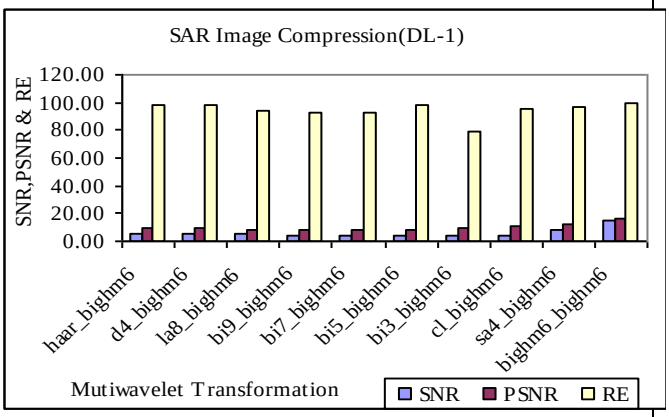

Fig. 2. (a) SNR, PSNR & RE at Decomposition Level-1.

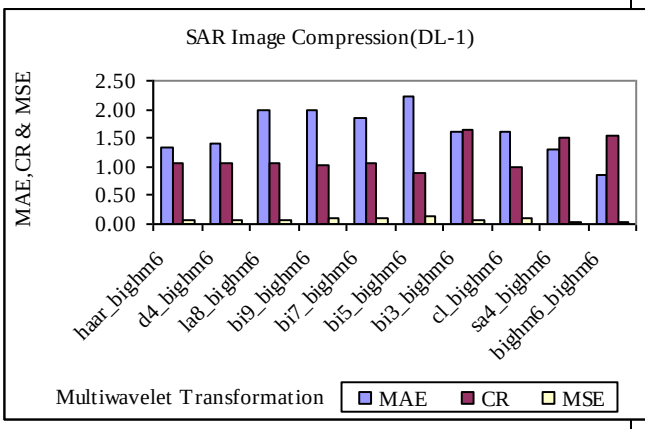

Fig. 2. (b) MAE, CR & MSE at Decomposition Level-1.

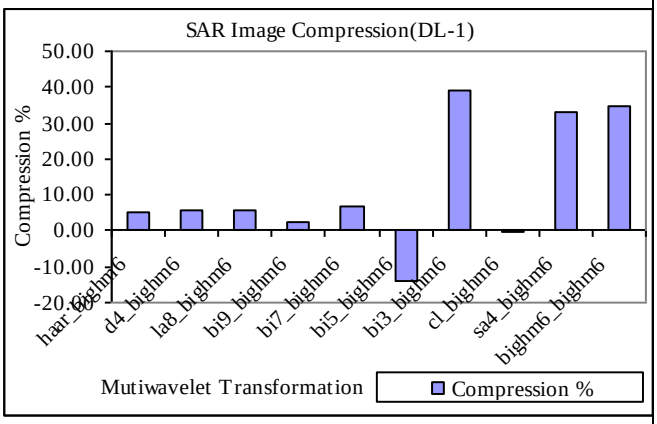

Fig. 2. (c) Compression in percentage at Decomposition Level-1.

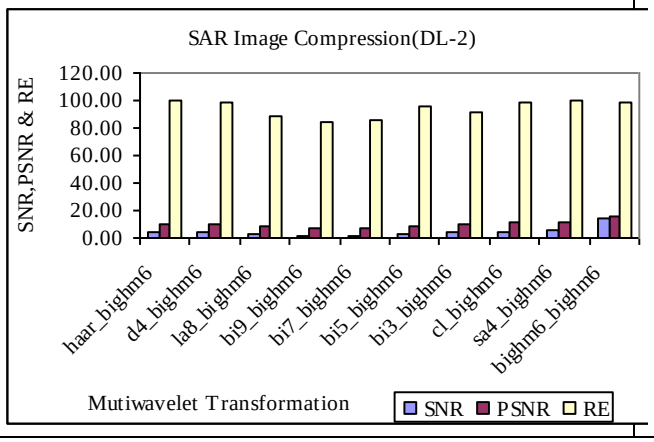

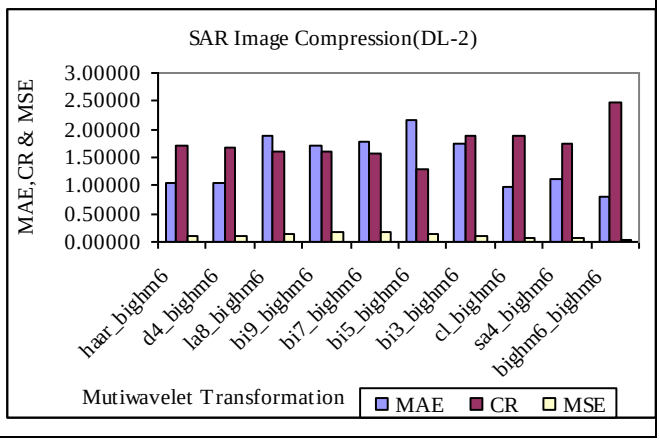

Fig. 2. (d) SNR, PSNR & RE at Decomposition Level-2.

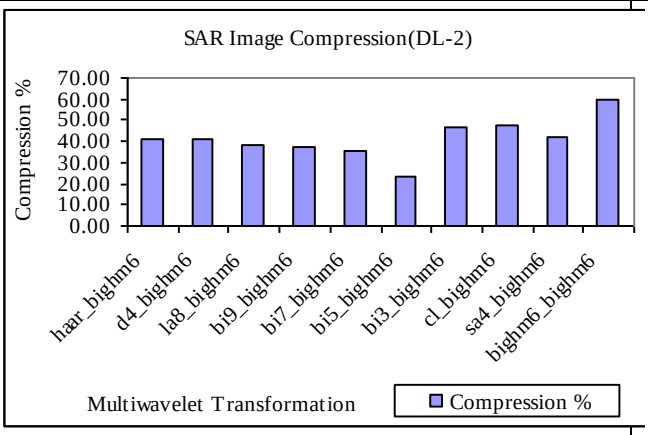

Fig. 2. (e) MAE, CR & MSE at Decomposition Level-2.

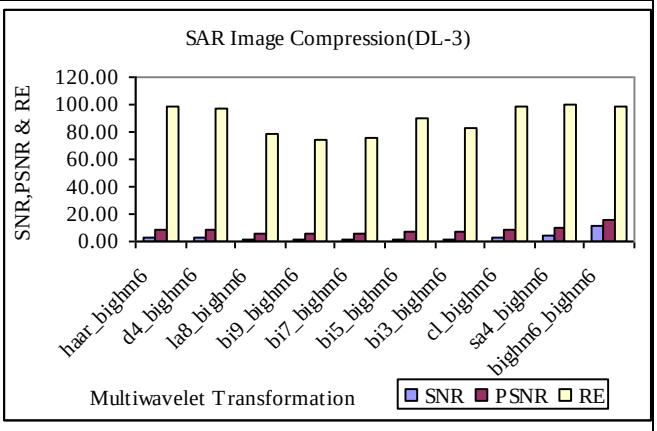

Fig. 2. (f) Compression in percentage at Decomposition Level-2.

Fig. 2. (g) SNR, PSNR & RE at Decomposition Level-3.

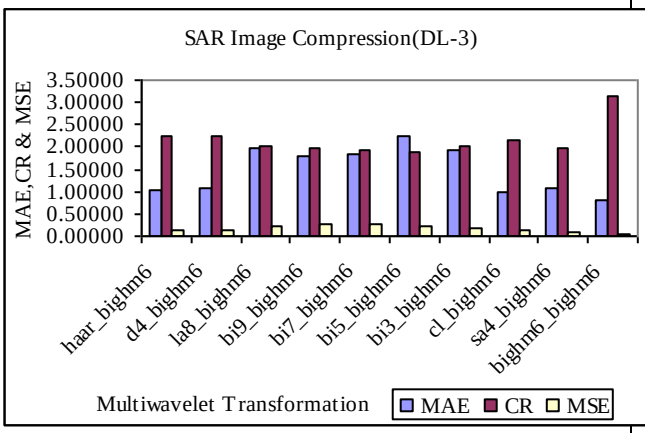

Fig. 2. (h) MAE, CR & MSE at Decomposition Level-3.

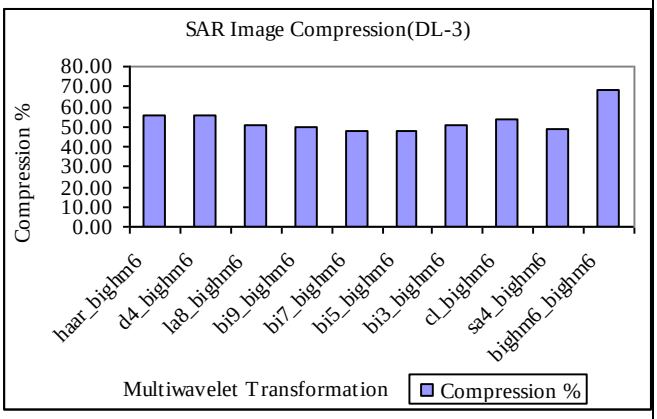

Fig. 2. (i) Compression in percentage at Decomposition Level-3.

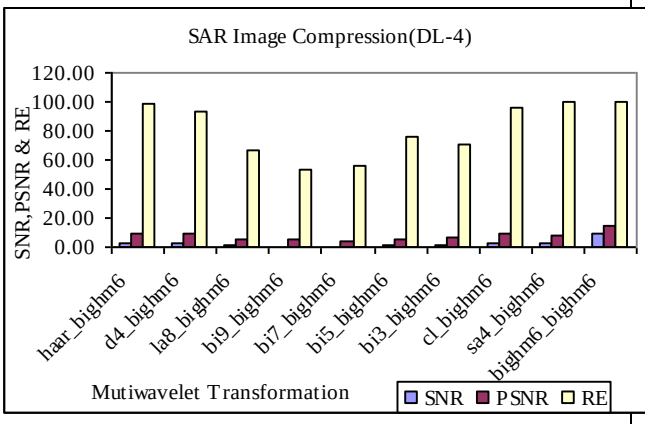

Fig. 2. (j) SNR, PSNR & RE at Decomposition Level-4.

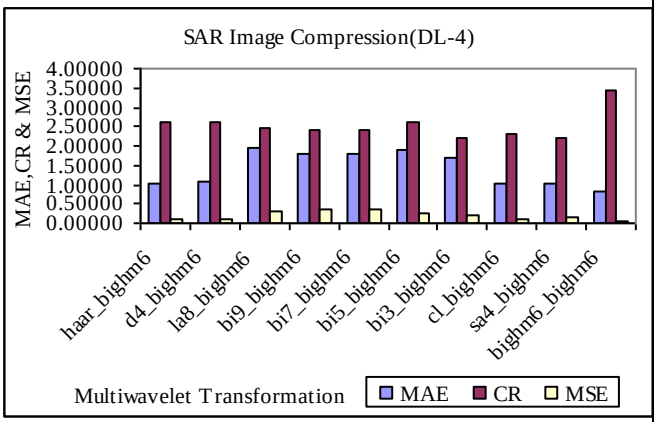

Fig. 2. (k) MAE, CR & MSE at Decomposition Level-4.

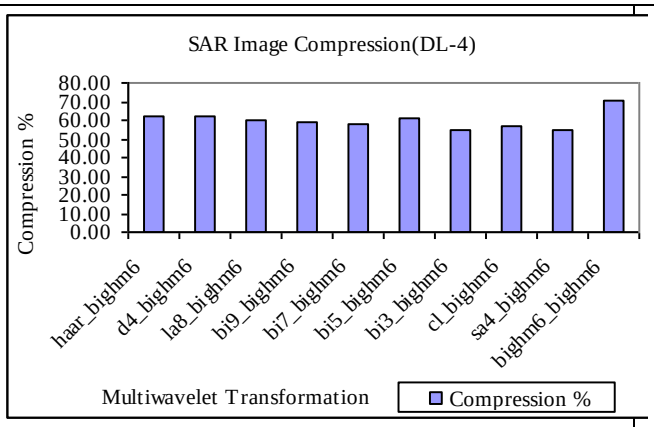

Fig. 2. (l) Compression in percentage at Decomposition Level-4.

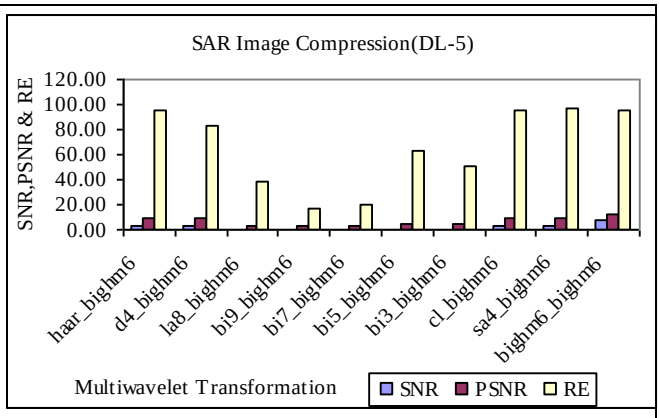

Fig. 2. (m) SNR, PSNR & RE at Decomposition Level-5.

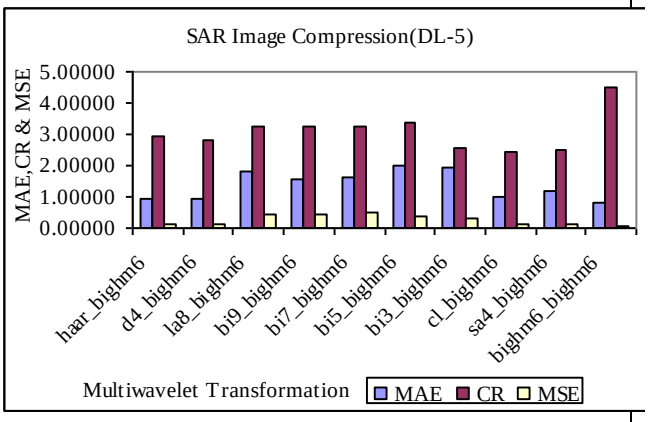

Fig. 2. (n) MAE, CR & MSE at Decomposition Level-5.

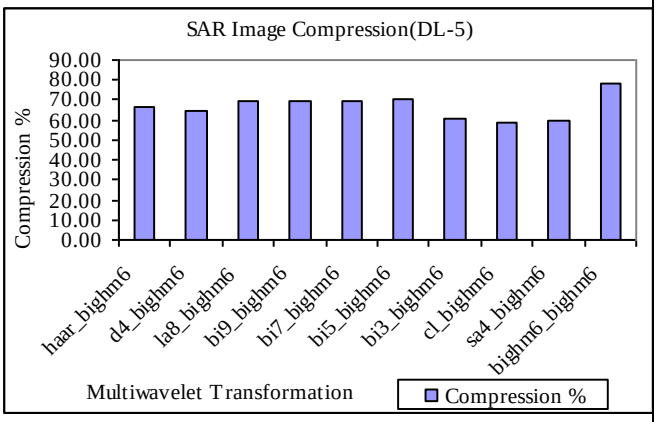

Fig. 2. (o) Compression in percentage at Decomposition Level-5.

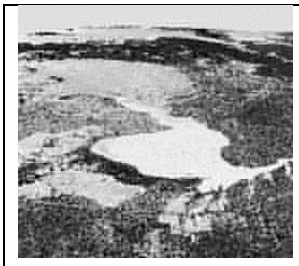

Fig 3. (a) Ival4.jpg original SAR image [256x256]

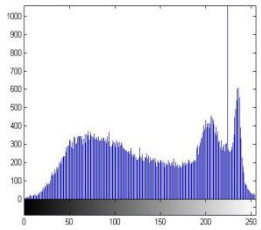

Fig 3. (b) Histogram of fig3.(a)

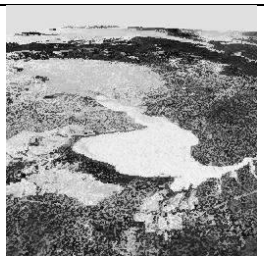

Fig 3. (c) compressed Image using BTC

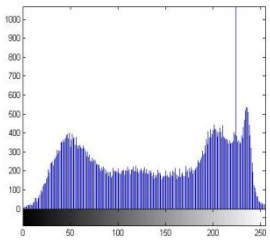

Fig 3. (d) Histogram of fig3.(c)

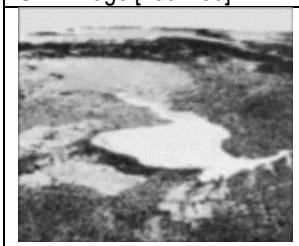

Fig 3. (e) compressed Image using GP

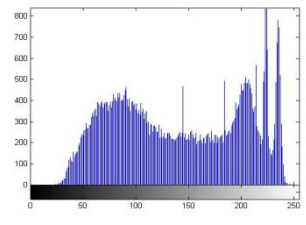

Fig 3. (f) Histogram of fig3.(e)

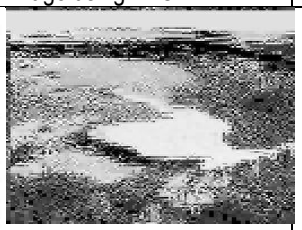

Fig 3. (g) compressed Image using haar

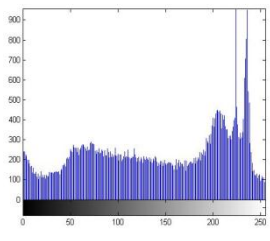

Fig 3. (h) Histogram of fig3.(g)

	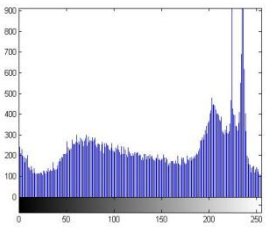		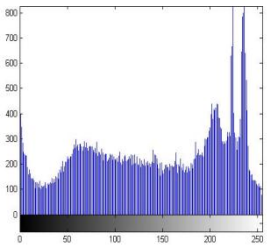
Fig 3. (i) compressed Image using D4	Fig 3. (j) Histogram of fig3.(i)	Fig 3. (k) compressed Image using La8	Fig 3. (l) Histogram of fig3.(k)
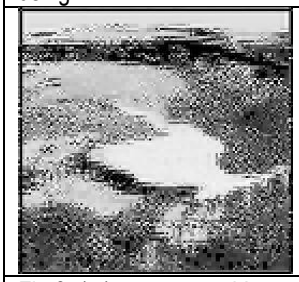	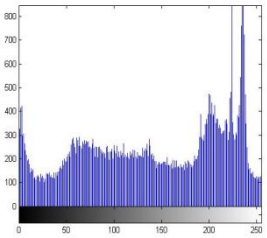		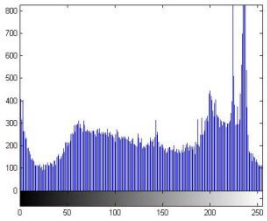
Fig 3. (m) compressed Image using Bi9	Fig 3. (n) Histogram of fig3.(m)	Fig 3. (o) compressed Image using Bi7	Fig 3. (p) Histogram of fig3.(o)
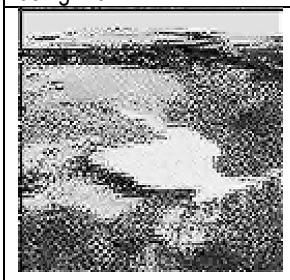	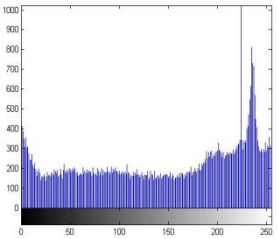	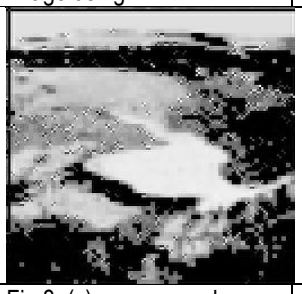	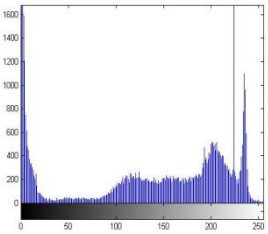
Fig 3. (q) compressed Image using Bi5	Fig 3. (r) Histogram of fig3.(q)	Fig 3. (s) compressed Image using Bi3	Fig 3. (t) Histogram of fig3.(s)
	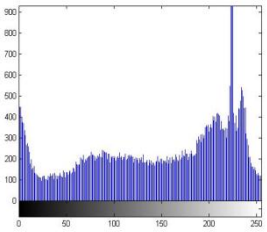	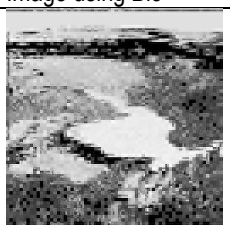	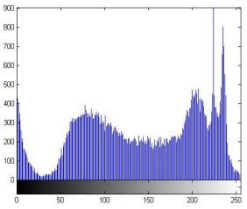
Fig 3. (u) compressed Image using CI	Fig 3. (v) Histogram of fig3.(u)	Fig 3. (w) compressed Image using Sa4	Fig 3. (x) Histogram of fig3.(w)
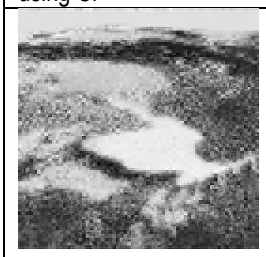	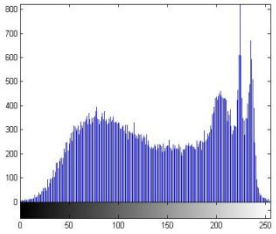		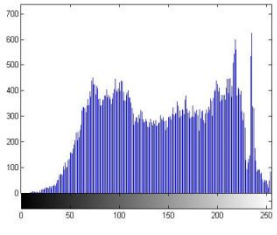
Fig 3. (y) compressed Image using Bighm6L1	Fig 3. (z) Histogram of fig3.(y)	Fig 3. (aa) compressed Image using Bighm6L3	Fig 3. (ab) Histogram of fig3.(aa)